Inorganic Chemistry

ARTICLE

pubs.acs.org/IC

Chalcogenophilicity of Mercury

Abu Md. Asaduzzaman* and Georg Schreckenbach*

Department of Chemistry, University of Manitoba, Winnipeg, Manitoba R3T 2N2, Canada

Supporting Information

ABSTRACT: Density-functional theory (DFT) calculations have been carried out to investigate the chalcogenophilicity of mercury (Hg) reported recently [*J. Am. Chem. Soc.* **2010**, *132*, 647−655]. Molecules of different sizes have been studied including ME, $[M(EH)_4]^n$, $M(SH)_3EH$ (M = Cd, Hg; E = S, Se, Te; n = 0, 2+) and $[Tm^Y]MEZ$ complexes (Tm = tris(2-mercapto-1-*R*-imidzolyl)hydroborato; Y = H, Me, Bu^t; M = Zn, Cd, Hg; E = S, Se, Te; Z = H, Ph). The bonding of Cd and Hg in their complexes depends on the oxidation state of the metal and nature of the ligands. More electronegative ligands form bonds of ionic type with Cd and Hg while less electronegative ligands form bonds that are more covalent. The Cd-ligand bond distances are shorter for the ionic type of bonding and longer for the covalent type of bonding than those of the corresponding Hg-ligand bonds. The variation of this Cd/Hg bonding is in accordance with the ionic and covalent radii of Cd and Hg. The experimentally observed (shorter) Hg−Se and Hg−Te bond distances in $[Tm^{Bu^t}]$HgEPh (E = S, Se, Te) are due to the lower electronegativity of Se and Te, crystal packing, and the presence of a very bulky group. The bond dissociation energy (BDE) for Hg is the highest for Hg−S followed by Hg−Se and Hg−Te regardless of complex type.

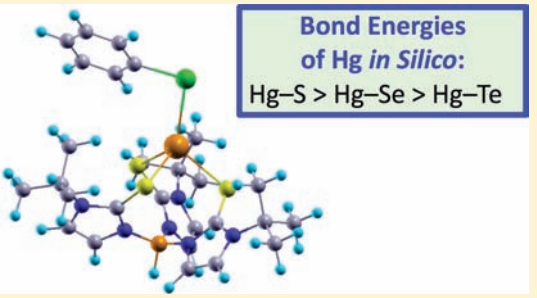

INTRODUCTION

Mercury has been well-known as a toxic element for centuries.[1] The toxicity of Hg has received much more scientific attention than ever before since the report of the Minamata disease[2,3] in Japan. The toxicity of mercury is attributed to the binding affinity of mercury to the sulfur atom of cysteine and methionine residues in proteins and enzymes.[4−11] While mercury−sulfur bonding is believed to be the foundation for the mercury toxicity in biological systems, the mercury−selenium bonding in selenoproteins, which is often present in the cysteine and methionine residues (selenocysteine and selenomethionine) represses the toxicity of mercury. This process is known as the mercury−selenium antagonism.[12−15] The antagonism phenomena in the animal body have been known for decades although the mechanism is not clear and often subject of intense debate. Some studies propose that the stronger mercury−selenium binding[16−19] compared to the mercury−sulfur bond is the probable reason for the mercury−selenium antagonism. Other studies, however, suggest that the mercury−sulfur bond is, in fact, stronger than the mercury−selenium bond.[20−23]

To identify the origin of the antagonism phenomena, we have recently reported the synthesis of methyl mercury complexes of four selenoamino acids followed by a detailed computational study of methyl mercury complexes of both amino and selenoamino acids.[20,24] In these studies, we have investigated the mercury−sulfur and mercury−selenium bonding in their respective complexes in some detail. From a variety of characterization techniques, we have concluded that, in related complexes, the mercury−sulfur bond is stronger than its mercury−selenium analogue. In this context, a very recent article by Melnick and coworkers[25] caught our attention. These authors have synthesized a series of zinc, cadmium, and mercury chalcogenolate complexes. The article has been highlighted in Chemical and Engineering News,[26] further illustrating the importance of the Hg toxicity and of the Hg−Se antagonism. Here we report a computational approach to provide a better understanding of the interactions between mercury and chalcogens.

The term chalcogenophilicity is used here as to describe the affinity of mercury toward chalcogens. The affinity thus is represented by the absolute bonding energy of mercury with chalcogens.

COMPUTATIONAL PROCEDURE

Calculations were performed with the Priroda code (version 6)[27−29] in the framework of density-functional theory (DFT).[30] The generalized-gradient approximation functional PBE[31] was employed for these Priroda calculations. Priroda applies a scalar four-component relativistic method[32] with all electron basis sets. For all atoms, extensive correlation consistent triple-ζ-polarized quality basis sets[28] for the large component, corresponding kinetically balanced basis sets for the small component, and appropriate auxiliary (fit) basis sets were employed.[28] We have shown earlier[20,33−36] that our present computational protocol characterizes organometallic systems and other heavy metal complexes well. For all optimized structures of complexes, their nature as true local energy minima was verified by calculating the analytical harmonic

Received: January 28, 2011
Published: March 15, 2011

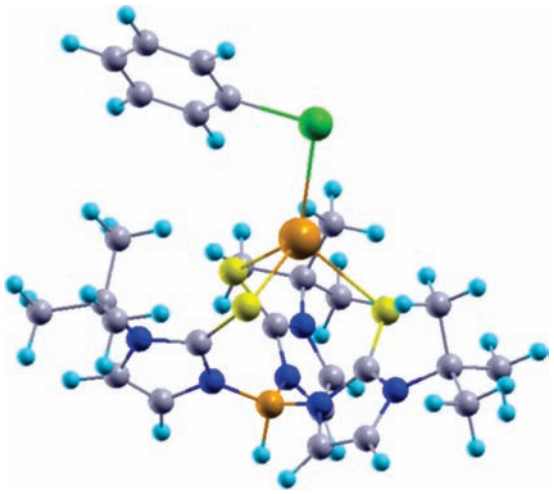

Figure 1. Ball and stick representation of the optimized structure of the [Tm^{Bu^t}]HgTePh complex. The structures for other complexes (Zn and Cd instead of Hg, and S and Se instead of Te) are qualitatively similar. The gray, blue, yellow, small orange and light blue, green and big orange balls correspond to C, N, S, B, H, Te, and Hg atoms, respectively.

frequencies. Bond decomposition[37,38] analysis was carried out using the ADF code[39−43] with PBE and small-core triple-ζ-basis sets (ZORA-TZ2P). Relativistic effects were treated using the Zeroth Order Regular Approximation (ZORA) to the Dirac equation with spin−orbit operator.[44,45]

RESULTS AND DISCUSSION

Experimental Work on [Tm^{Bu^t}]MEPh. Before presenting our results, we would like to revisit the work of Melnick and co-workers.[25] These authors synthesized chalcogenolate complexes [Tm^{Bu^t}]MEPh, with M = Zn, Cd, Hg; E = S, Se, Te and *Tm* = tris(2-mercapto-1-*R*-imidzolyl)hydroborato as shown in Figure 1. From X-ray crystallography, the M−Tm^{Bu^t} and M−EPh bond distances have been determined. In the case of the M−Tm^{Bu^t} distances, they obtained the bond distances as Zn−S < Cd−S < Hg−S in a monotonic fashion in all three chalcogenolate complexes. (Note that only M−S bonds are considered in this case.) However, for the MEPh part they obtained the bond distances in the order of Zn−E < Hg−E < Cd−E for all three chalcogens. Probably the most striking feature of the article is the difference in bond distance between Cd−EPh and Hg−EPh, from which the authors derived that the chalcogenophilicity of Hg increases in the sequence S < Se, Te.

We, however, would like to pinpoint another feature that we feel needs to be considered and discussed. While the Cd−EPh bond distances are longer than Hg−EPh as they presented (in Figure 5 of ref 25), the Cd−S(Tm^{Bu^t}) bond distances are actually *shorter* than Hg−S(Tm^{Bu^t}) in the same complexes as shown in Figure 4 of ref 25. (This has been briefly noted by the authors of ref 25 but without any discussion.) In our opinion, these contradicting trends of bond distances (one Cd−S bond is longer, whereas the other three are shorter compared to the corresponding distances of Hg in the similar complexes) need to be explained before drawing any conclusions regarding the chalcogenophilicity of Hg. We will show this in this paper. In doing so, a systematic approach has been adopted where the smallest molecules containing M−E bonds are studied first, followed by the gradual increment of molecular size up to the experimental molecules. In this way, the effect of the ligands' structure and number on the M−E bond will be addressed.

Table 1. M−L Bond Distances (L = E, Cl, Br, I, EH; E = S, Se, Te; M = Cd, Hg; in Å) in Selected Molecules[a]

complexes	Cd−L	Hg−L
MS	2.2484 (2.250)	2.2485 (2.252)
MSe	2.3673 (2.361)	2.3784 (2.377)
MTe	2.5583 (2.546)	2.5764 (2.574)
$[MCl_4]^{2-}$	2.5479 (2.458)	2.5920 (2.487)
$[MBr_4]^{2-}$	2.6895 (2.585)	2.7284 (2.608)
$[MI_4]^{2-}$	2.8872 (2.779)	2.9129 (2.784)
$[M(SH)_4]^{2-}$	2.6266	2.6581
$[M(SeH)_4]^{2-}$	2.7453	2.7726
$[M(TeH)_4]^{2-}$	2.9246	2.9326
$M(SH)_4$	2.4244	2.4055
$M(SeH)_4$	2.5527	2.5385
$M(TeH)_4$	2.7495	2.7342

[a] The values in parentheses are literature values.[25,46,47]

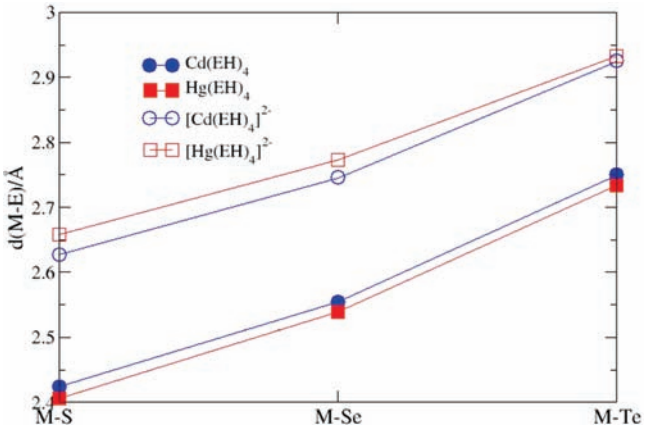

Figure 2. Calculated M−E bond distances for $[M(EH)_4]^n$; *n* = 0, 2-, M = Cd, Hg, E = S, Se, and Te.

M−E Bonds in Small Model Complexes. Since the goal of the current study is a detailed investigation of the chalcogenophilicity of Hg, we have not always included Zn complexes, especially for the study of small molecules, although we have done so for the bigger molecules that are directly related to the recent work of Melnick et al.[25] The optimized metal−ligand bond distances of the small molecules that we have considered are summarized in Table 1.

Our calculated Cd−E and Hg−E bond distances and trends for ME (E = S, Se, Te; M = Cd and Hg) are in very good agreement with the results of Peterson and co-workers[23] who carried out very high level theoretical calculations on group 12 metal chalcogenides. The M−L bond distances and trends for the halogen complexes are also in agreement with an earlier report.[46]

Looking at the values in Table 1, we notice two principal types of bond distances in the molecules containing Cd and Hg atoms. For the first nine sets of molecules in Table 1, we find that the Cd−L/E bond distances are shorter compared to the Hg−L/E distances. However, for the last three molecules [$M(EH)_4$, E = S, Se, Te], we have observed the opposite trend, that is, the Cd−E

dx.doi.org/10.1021/ic200199b |*Inorg. Chem.* 2011, 50, 3791–3798

bond distances are longer than the corresponding Hg−E bonds. Focusing on ($[M(EH)_4]^n$; n = 0 and 2-) alone, two contradicting M−E bond distance trends are observed. For n = 2-, the Cd−E bond distances are shorter whereas, for n = 0, the Cd−E distances are longer than the Hg−E distances, respectively, as shown Figure 2.

We would like to emphasize that, for n = 2-, the complexes have two possible structural isomers, that is, tetrahedral and square planar. The tetrahedral structures are the most stable isomers and are presented here accordingly. However, for n = 0, we have obtained only square planar structures for both Cd and Hg complexes. A starting geometry with tetrahedral arrangement for n = 0 always optimized to the square planar structures. Generally, square planar complexes are obtained only when the "ligand field stabilization", that is, the covalent contribution, exceeds the electrostatic repulsion between the negatively charged ligands (and/or the steric repulsion). On the other hand, a purely electrostatic and steric picture leads to the tetrahedral structure since this maximizes the distance between the ligands. According to the crystal field theory, transition elements with $4d^8$ and $5d^8$ electronic configurations will predominately possess square planar structures. For complexes with n = 2-, the electronic configuration is more likely d^{10}, and for n = 0, the electronic configuration is more likely d^8. The d^{10} electronic configuration facilitates the simple ionic type of bonding with a tetrahedral coordination. The d^8 electronic configuration, on the other hand, gives rise to the square planar structure. In summary, we observe opposite trends for the bond distances, depending on the charge state (formal d occupancy) of the complex, and we conclude that the M−E bond lengths might not be the sole criteria in evaluating the chalcogenophilicity of Hg.

Moreover, shorter bond distances do not always represent stronger bonds as shown by Gorelsky et al.[48] on a series of thiolate complexes of first row transition metals. Shorter bond distances result from higher orbital interactions, which depend on the energy of the interacting atomic orbitals. The orbital interaction is higher for the narrowing energy difference between interacting atomic orbitals.

Before further discussing these two apparently contradicting trends in bond lengths for Cd and Hg chalcogenides, let us first look at the Hg-chalcogen bond strengths available in the literature. Filatov et al.,[22] Cremer, et al.,[21] and Peterson et al.[23] carried out theoretical calculations on Hg chalcogenides. In their high-level calculations, they found that the bonding strength follows the sequence Hg−S > Hg−Se > Hg−Te. There are other studies related to systems involving bonds to S and Se; specifically involving E−H,[49] E−C,[49] E−P,[50] and E−TM bonds[51−53] (TM = transition metal). In each case, it was reported that the bond involving S is stronger than that involving Se. There are, however, a few other studies[16−19,54] which reported that the bonding involving Se is stronger than the corresponding S bonds. Among these studies, Sugira et al.[18,19] deduced that the Hg−Se bonds should be stronger, based on the observed Hg−S and Hg−Se distances. According to these authors, the observed Hg−Se bond distances were slightly shorter than what would be expected from the covalent radius of Se. As already mentioned, such a slight shortening of bond distances, however, is not always an indication of a stronger bond.[20,48] Subtle increases in the orbital interactions often lead to a slightly shorter bond distance. We have discussed this issue in our earlier paper.[20] The others two papers[16,17] that concluded that the Hg−Se is stronger than the Hg−S bond were based on the measurement of formation constants. However, a higher value of the formation constant is not necessarily an indication of a particular type of bond being stronger. The formation constant is a relative energetic term that depends on the energy of reactants *and* products. For instance, while the formation constant of methyl mercury selenoamino acid complexes is higher than that of the corresponding methyl mercury amino acid complexes, the bond strength of Hg−S is stronger than that of Hg−Se in the respective complexes. The higher formation constant for Se containing complexes is due to the instability of the selenoamino acids (the reactants) rather than the strength of the Hg−Se bonding.[20] Another paper[54] which reported the Fe−Se bonding being stronger than Fe−S is based on semiempirical Hückel molecular orbital calculations.[55−57] In this particular study,[54] the geometries were not optimized; rather, single point molecular calculations were performed at the geometries taken from the average structural parameters from crystal structures.

Now, let us return to the bond distances of Hg and Cd with different ligands. The chemical bonding in any complex is usually described by the covalent and ionic interactions. In general, the strength of covalent bonding depends on the extent of overlap between two interacting atomic orbitals. The strength of ionic bonds, on the other hand, depends on the electronegativity difference between the interacting atoms and hence the charge on the individual atoms in molecules. There is, however, a continuous change from ionic to covalent and vice versa, and hence it is very difficult to draw an unambiguous borderline between them. All those molecules/complexes[21−23,46] for which the Hg−E bond is found to be longer than the corresponding Cd−E bond have the metal (Cd or Hg) in its formal 2+ oxidation state (d^{10}). If we consider ionic bonding as dominant in those complexes having Cd and Hg in their 2+ oxidation state (d^{10}), then the M−E bond distances are in accordance with the ionic radii of Hg and Cd; longer bond distances involving Hg, which has the larger ionic radius (Pauli's ionic radii for Cd(II) and Hg(II) are 97 and 110 pm,[58] respectively). On the other hand, in a compound where covalency is the dominant part of the bonding, that is, with less electronegative ligands, the Cd−E bond distances are longer than Hg−E according to the covalent radii 144 and 132 pm[58,59] of Cd and Hg, respectively. For example, in the $(Ph_3P)_2ML_2$ (M = Cd, Hg; L= Cl)[60,61] complexes, the Cd−L bonds are shorter than the Hg−L bonds, whereas the M−P bonds show the opposite trend. Looking at the atom linking to the metal, it can easily be deduced that the binding of the metal with the more electronegative chlorine atom is predominantly ionic and therefore the bond distances vary according to the ionic radii of Cd and Hg. On the other hand, phosphorus is much less electronegative and hence its bonding with the metal atom is of predominantly covalent type and behaves in accordance with the covalent radii of Cd and Hg. This experimental report actually is in agreement with our above-mentioned observations.

To mimic the experimental compounds and investigate the substitution effect, we have replaced one SH group in the $[M(SH)_4]^n$ complexes (n = 0, 2-) by an SeH and TeH group, respectively, and obtained $[M(SH)_3SeH]^n$ and $[M(SH)_3TeH]^n$. For n = 2-, the trend in the M−E bond distances (E = S, Se, Te) for the substituted complexes is very much similar to that for the unsubstituted complexes (see the Supporting Information, Figure S1). However, the pattern of the M−E bond distances for n = 0 in the substituted complexes is different from that of the

dx.doi.org/10.1021/ic200199b |*Inorg. Chem.* 2011, 50, 3791–3798

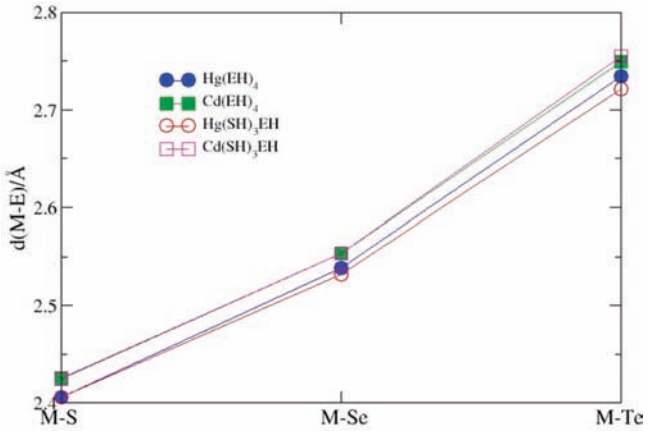

Figure 3. M−E bond distances for $M(SH)_3EH$; E = S, Se, Te and M = Cd and Hg. For comparison those for $M(EH)_4$ are also shown.

Table 2. M−E Bond Distances (Å) for $M(SH)_3EH$ (E = S, Se, Te; M = Cd, Hg)[a]

	$M(SH)_3EH$		$M(EH)_4$	
	Hg	Cd	Hg	Cd
S	2.4055	2.4244	2.4055	2.4244
Se	2.5316	2.5532	2.5385	2.5527
Te	2.7213	2.7547	2.7342	2.7495

[a] For comparison, those for $M(EH)_4$ are also presented.

Table 3. BDE (kcal/mol) for M−E Bonds in $[M(EH)_4]$ (M = Cd, Hg; E = S, Se, Te)

		BDE (per M−E bond[a])		
no.	reaction	S	Se	Te
1	$Cd(EH)_4 \rightarrow Cd + 4EH$	33.95	30.87	27.64
2	$Cd(SH)_3EH \rightarrow Cd(SH)_3 + EH$	34.31	30.54	26.96
3	$Hg(EH)_4 \rightarrow Hg + 4EH$	30.86	27.52	24.43
4	$Hg(SH)_3EH \rightarrow Hg(SH)_3 + EH$	43.47	39.44	35.39

[a] Average BDE of the M−E bond, i.e., reaction free energy of reactions 2 and 4, and 1/4 of the reaction energy for reactions 1 and 3.

unsubstituted complexes as shown in Figure 3 and Table 2. For the unsubstituted complexes, the difference between Cd−E and Hg−E is almost similar for all three chalcogenides, leading to essentially parallel lines in Figure 3 (filled blue circles and filled green squares, respectively). However, in the substituted complexes the Cd−E and Hg−E bond distances (E = Se and Te) vary in an opposite way. The Cd−Se and Cd−Te bond distances are longer in the substituted complexes than those in the unsubstituted complexes, whereas, the Hg−Se and Hg−Te bond distances are shorter in the substituted complexes than those in the unsubstituted complexes. For both metal atoms, the deviation of bond distance in the substituted complexes is higher for Te than that for Se. The opposite trends variation of the M−E bond distances leaves the largest difference between Cd−Te and Hg−Te, followed by Cd−Se/Hg-Se and Cd−S/Hg-S. This situation agrees nicely with the main feature of the article by Melnick et al.[25]

Table 4. Interaction Energy (kcal/mol) between $HgSH^+$ and EH^- in Hg(SH)EH (E = S, Se, and Te)

energy	$Hg(SH)_2$	Hg(SH)SeH	HgTeH
total	−226.04	−221.65	−215.31
Pauli repulsion	148.67	139.00	133.02
electrostatic interactions	−263.72	−248.62	−232.89
orbital interactions	−110.99	−112.03	−115.94

Next, let us have a look at the energetic picture for the above situation. We have summarized the calculated bond dissociation energies (BDE) in Table 3.

For both Hg and Cd, the M−E BDE is getting smaller as we are moving from S to Se to Te, Table 3. This finding regarding the trend of the BDE is in agreement with the literature.[21−23] The Cd−E BDEs for the two sets of reactions differ slightly. For the substituted complexes (reaction 2), we have obtained slightly smaller BDEs compared to those of the unsubstituted complexes (reaction 1). This observation is in accordance with the increase of the bond distances as we show in Figure 3. The slightly longer Cd−E bond lengths in the substituted complexes result from slightly smaller binding energies. In the substituted complexes, the EH group (E = Se and Te) competes with the other three SH groups. The more electronegative SH interacts slightly stronger and thus weakens the Cd−Se and Cd−Te bonds. The weaker Cd−Se and Cd−Te bonds become slightly longer. However, the BDEs for Hg−E of the substituted complexes are higher than those of the unsubstituted systems, which result in shorter bond lengths as seen in Figure 3. Thus, we observe opposite bonding patterns between Hg and Cd. However, this unusual behavior of Hg does not provide any proof for a higher affinity of Hg toward Te or Se over S atoms. It is known that, the higher the difference in electronegativity of the interacting atoms, the more ionic in character the bond between them will be. Along the same line of argument, a smaller difference in the electronegativity of the interacting atoms will lead to a more covalent bonding. The Pauling electronegativity values for Hg and Te are 2.0 and 2.1,[58] respectively. They have the smallest difference among all the interacting pairs of atoms in the $M(EH)_4$ series. Therefore, we would expect to have a covalent (or coordination) bond between Hg and Te according to the electronegativity picture. Moreover, relativistic effects play a major role in both Hg and Te. Indeed, Hg is known as a "relativistic maximum" within the periodic table.[62]

To provide quantitative discussions, we have performed a Ziegler−Morokuma bond decomposition analysis[37,38,63] on a simple Hg(SH)EH system. In this formalism, the bond formation energy is decomposed into two terms, (i) the strain energy that is required for the deformation of the fragments from their equilibrium geometries to those in the molecules and (ii) the interaction energy. The interaction energy is further decomposed into (a) repulsive Pauli energy, (b) attractive electrostatic energy and (c) attractive orbital interaction energy. Since our goal is to differentiate the electrostatic and orbital interactions, we have left out the strain energy. Considering the $HgSH^+$ and EH^- as fragments, the calculated interaction energy is tabulated in Table 4.

It is clear from the Table 4 that the two types of attractive forces between Hg and chalcogen atoms vary in opposite ways, that is, the electrostatic interaction is higher for the more electronegative chalcogen and the orbital interaction is higher for the less electronegative chalcogen. The gain of orbital interaction with less electronegative chalcogen atoms, however,

dx.doi.org/10.1021/ic200199b |*Inorg. Chem.* 2011, 50, 3791–3798

Table 5. Optimized M−EY (Y = H, Ph) and M−Tm^X (X = H, Me, Bu^t) Bond Distances (Å) in [*Tm*$^{Bu^t}$]MEY Complexes (M = Zn, Cd, Hg; E = S, Se, Te)

	[Tm^H]MSPh		[Tm^H]MSePh		[Tm^H]MTePh	
	M−SPh	M−[Tm^H]$_{av}$	M−SePh	M−[Tm^H]$_{av}$	M−TePh	M−[Tm^H]$_{av}$
Zn	2.2558	2.4126	2.3765	2.4146	2.5660	2.4169
Cd	2.4491	2.6329	2.5600	2.6373	2.7343	2.6413
Hg	2.4352	2.6872	2.5448	2.6933	2.7072	2.7000
	[Tm^{Me}]MSPh		[Tm^{Me}]MSePh		[Tm^{Me}]MTePh	
	M−SPh	M−[Tm^{Me}]$_{av}$	M−SePh	M−[Tm^{Me}]$_{av}$	M−TePh	M−[Tm^{Me}]$_{av}$
Zn	2.2602	2.4044	2.3842	2.4089	2.5741	2.4102
Cd	2.4555	2.6250	2.5661	2.6297	2.7404	2.6332
Hg	2.4399	2.6804	2.5507	2.6888	2.7110	2.6940
	[*Tm*$^{Bu^t}$]MSPh		[*Tm*$^{Bu^t}$]MSePh		[*Tm*$^{Bu^t}$]MTePh	
	M−SPh	M−[*Tm*$^{Bu^t}$]$_{av}$	M−SePh	M−[*Tm*$^{Bu^t}$]$_{av}$	M−TePh	M−[*Tm*$^{Bu^t}$]$_{av}$
Zn	2.2693	2.3988	2.3876	2.4006	2.5776	2.4021
Cd	2.4585	2.6127	2.5696	2.6220	2.7441	2.6254
Hg	2.4449	2.6716	2.5553	2.6775	2.7156	2.6835
	[Tm^H]MSH		[Tm^H]MSeH		[Tm^H]MTeH	
	M−SH	M−[Tm]$_{av}$	M−SeH	M−[Tm]$_{av}$	M−TeH	M−[Tm]$_{av}$
Zn	2.2437	2.4194	2.3688	2.4187	2.5631	2.4175
Cd	2.4345	2.6392	2.5504	2.6406	2.7306	2.6416
Hg	2.4237	2.6894	2.5391	2.6924	2.7055	2.6960
	[*Tm*$^{Bu^t}$]MSH		[*Tm*$^{Bu^t}$]MSeH		[*Tm*$^{Bu^t}$]MTeH	
	M−SH	M−[*Tm*$^{Bu^t}$]$_{av}$	M−SeH	M−[*Tm*$^{Bu^t}$]$_{av}$	M−TeH	M−[*Tm*$^{Bu^t}$]$_{av}$
Zn	2.2524	2.4071	2.3784	2.4061	2.5738	2.4041
Cd	2.4421	2.6254	2.5585	2.6262	2.7391	2.6266
Hg	2.4318	2.6756	2.5476	2.6778	2.7136	2.6806

is not sufficient to offset the much stronger electrostatic interactions for higher electronegative chalcogen atoms. As a net result, therefore, the Hg−S bond is the strongest followed by the Hg−Se and Hg−Te bonds.

[*Tm*$^{Bu^t}$]MEPh and Related Complexes. From the smaller, related systems, we will now turn to the large systems that Melnick et al.[25] studied (Figure 1). We also include some other, closely related complexes that are less sterically hindered. The calculated M−E bond distances (M = Zn, Cd, Hg; E = S, Se, Te) are summarized in Table 5.

We have obtained two contradicting trends in the bond distances for these complexes, similar to the previously discussed data for small molecules, as shown in Figures 4 and 5. These trends are also apparent in the X-ray data of Melnick et al.[25] The M−Tm bond distances (see Figure 4) are monotonic and follow the order Hg-*Tm*$^{Bu^t}$> Cd-*Tm*$^{Bu^t}$> Zn-*Tm*$^{Bu^t}$, similar to that found by Melnick et al.[25] Moreover, we have obtained a variation in the M−EPh bond distances that is also similar to the experimental trend, as shown in Figure 5 (specifically Cd−EPh > Hg−EPh > Zn−EPh).

The calculated M−*Tm*$^{Bu^t}$ and M−EPh bond distances are within 3−4% and 1% of their experimental values, respectively, Table 5 and Figures 4 and 5. The somewhat larger deviation of our calculated M−*Tm*$^{Bu^t}$ bond lengths might result from two possible sources, (i) the repulsive interactions between the large *Tm*$^{Bu^t}$ ligands and the phenyl group and (ii) a lack of crystal packing in our models and hence the absence of some intermolecular interactions. We have probed the first point by

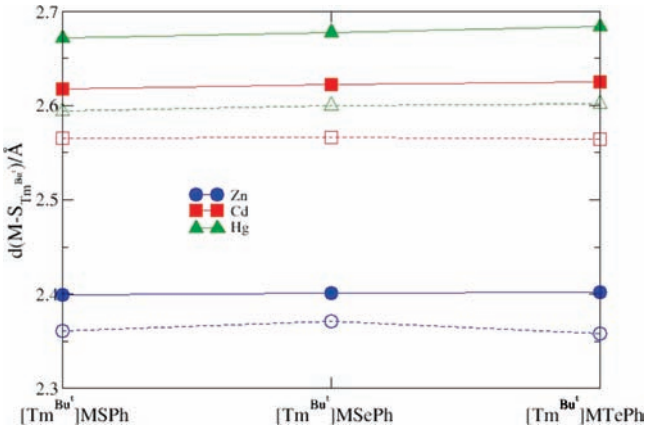

Figure 4. M−S(*Tm*$^{Bu^t}$) bond distances in [*Tm*$^{Bu^t}$]MEPh (M = Zn, Cd, Hg; E = S, Se, Te) complexes. The dashed lines with open symbols are for corresponding (same color) experimental values.[25]

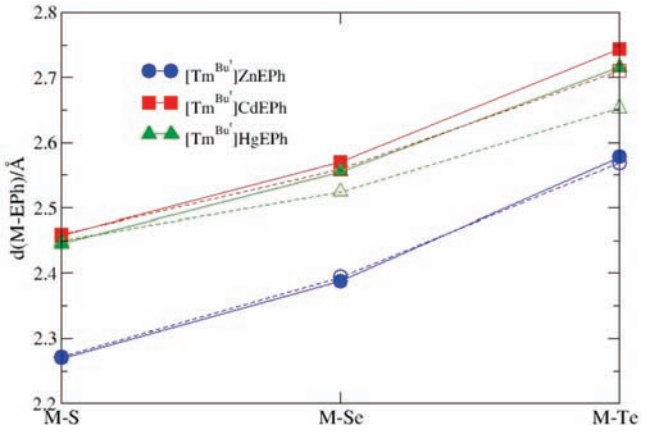

Figure 5. M−EPh bond distances in [*Tm*$^{Bu^t}$]MEPh (M = Zn, Cd, Hg; E = S, Se, Te) complexes. The dashed lines with open symbols are for corresponding (same color) experimental values.[25]

replacing (a) the t-butyl groups of Tm by H, (b) the same t-butyl groups by methyl groups, (c) the phenyl ring by H atoms, and (d) both the t-butyl and phenyl groups by H atoms. The calculated M−Tm and M−EPh(H) bond distances for situations (a), (b), (c), and (d) are shown in Table 5. Looking at the table, we notice a contradicting trend in M−EPh(H) and M−Tm bond distances upon replacing the t-butyl group of the Tm ligand. The M−EPh bond distances are getting slightly longer along the series of increasing steric bulk at the Tm, H to CH_3 to t-butyl. The M−Tm bond distances, on the other hand, are getting shorter along this same series H to t-butyl. A similar trend is obtained for replacing the phenyl group by an H atom. These observations regarding the changes of bond distances can be explained by the steric interactions between the t-butyl and phenyl groups. The larger steric repulsion between the bigger groups (the t-butyl and phenyl groups) induces the observed lengthening of the M−EPh bonds. In this situation, the metal atoms feel more attractions from the three S atoms of the Tm ligand, resulting in shorter M−Tm bond distances. Such structurally induced bond distance alterations might also hint at the possible role of crystal packing on the structural parameters. The crystal packing effect is further verified by calculating the potential energy

dx.doi.org/10.1021/ic200199b |*Inorg. Chem.* 2011, 50, 3791–3798

Table 6. BDE[a] (kcal/mol) of Hg−EPh and Hg−EH for [Tm^{Y}]HgEZ (Y= H, Me, Bu^{t}; E = S, Se, Te; Z = H, Ph)

reactions	BDE (kcal/mol)		
	S	Se	Te
[Tm^{H}]HgEPh → [Tm^{H}]Hg + EPh	50.75	50.23	49.70
[Tm^{Me}]HgEPh → [Tm^{Me}]Hg + EPh	51.49	50.94	50.38
[*Tm*$^{Bu^t}$]HgEPh → [*Tm*$^{Bu^t}$]Hg + EPh	51.75	51.23	50.65
[Tm^{H}]HgEH → [Tm^{H}]Hg + EH	62.67	59.04	55.29
[*Tm*$^{Bu^t}$]HgEH → [*Tm*$^{Bu^t}$]Hg + EH	63.44	59.80	56.76
[Tm^{H}]HgEPh → [Tm^{H}]Hg^{+} + EPh^{-}	124.83	125.33	125.18
[Tm^{Me}]HgEPh → [Tm^{Me}]Hg^{+} + EPh^{-}	121.89	122.44	122.22
[*Tm*$^{Bu^t}$]HgEPh → [*Tm*$^{Bu^t}$]Hg^{+} + EPh^{-}	118.28	118.77	118.59
[Tm^{H}]HgEH → [Tm^{H}]Hg^{+} + EH^{-}	142.08	136.91	131.91
[*Tm*$^{Bu^t}$]HgEH → [*Tm*$^{Bu^t}$]Hg^{+} + EH^{-}	135.61	130.37	124.76

[a] The calculated BDE is for the electronic energy.

surface (PES) of HgE (see Supporting Information, Figure S2). It is clear from the figure that the flattest PES is for HgTe followed by HgSe and HgS, which confirms the maximum crystal packing effect for complexes containing Te followed by Se and S. In addition, taking the experimental standard deviation into consideration, the gap between calculated and experimental H−Tm bond distances is narrowed further.

Although we have found a similar pattern for the Cd−EPh and Hg−EPh bond distances, the difference between the Cd−EPh and Hg−EPh values (E = Se, Te) is not as pronounced as found by Melnick et al.[25] as can be seen in Figure 5. This might again be due to the neglect of intermolecular interactions (crystal packing) in our molecular calculations. The crystal packing effects can be further illustrated by considering the experimental Hg−Se−Ph and Hg−Te−Ph bond angles from the data of Melnick et al.[25] The Hg−Se−Ph and Hg−Te−Ph angles from the crystal structures are 102.9° and 101.3°, whereas our calculated values are 100.0° and 97.1°, respectively. Again, we attribute the difference to crystal packing effects as shown in the PES calculations.

As we discussed already, the bonding between a metal atom and its ligand(s) depends on the intricate electronic and geometric characteristics of the partner atoms/groups. Depending on the electronegative or electropositive nature of the partner atoms, the bond between them could be either ionic or covalent. Therefore, we need to be careful in devising an appropriate protocol for determining the BDE of M−EPh bonds involving Hg, Te, or Se, as will be discussed next. Since the debate regarding the bonding strength involves primarily Hg, we will restrict ourselves to discussing the BDE involving Hg only.

The BDE can be determined by either considering charged fragments ([*Tm*$^{Bu^t}$]M^{+} and EPh^{-}) or neutral fragments ([*Tm*$^{Bu^t}$]Hg and EPh). For Hg, where the nature of the bond strongly depends on the ligand environment in the complexes, it is very important to consider the right fragments for the calculation of the BDE. Moreover, in the earlier discussion on the bond distance trends between Cd−E and Hg−E, we have seen that the M−Tm bond distance varies according to the ionic radii of M whereas the M−EPh bond distance varies with the covalent radii of M. Therefore, we believe that calculating the BDE with neutral fragments would represent the true binding strength between Hg and E. We have, however, presented the BDE with both types of fragments for comparison as shown in Table 6.

For neutral fragments, we have obtained BDEs in the order Hg−S > Hg−Se > Hg−Te for the complexes, in accordance with previous reports.[21,22] While the Y (H, Me, Bu^{t}) group of Tm has little effect on the BDE, the Ph group has a significant impact on the BDE. In the complexes where Ph is substituted by an H atom, the BDE difference among the three complexes is more pronounced, Table 6.

In general, the BDE for charged fragments follows a similar trend as that of neutral fragments in those complexes where Ph is substituted. Only in Ph-group-containing complexes is the BDE for Se complex slightly higher (by ca. 0.5 kcal/mol) than that of S. However, the BDE for the Te complex is slightly smaller than that of Se. This reversed bonding energy from charged fragments actually arises because of the presence of EPh^{-} groups. The dependency of the BDE on the Ph group arises from the delocalization capability of the Ph group. While the electron affinity of EH (E = S, Se, Te) largely depends on the electronegativity of the E atoms as we have found in our calculations (see Supporting Information, Table S1), the electron affinity of the EPh group is essentially independent of the type of E atoms (Supporting Information, Table S1). The delocalization capability of the Ph group offsets the electronegativity of E. This delocalization might be responsible for the observed shorter Hg−Te bond distance. Another important point is that for both types of fragments, the difference of BDE between S, Se, and Te with the EH group is more pronounced than that with the EPh group. This might again be related to the conjugation or delocalization capacity of Ph group. This type of electronic characteristics of a particular group attached to the complexes might influence the particular bonding; however, it does not alter the relative bonding strength of Hg for S, Se, or Te, although it sufficiently reduces the gap between them. Thus, while the BDEs for the EH complexes follow the sequence Hg−S > Hg−Se > Hg−Te, the values for the EPh complexes follow the sequence Hg−S ≈ Hg−Se > Hg−Te. These trends are in accord with previous studies.[20−23] To verify the basis set superposition error (BSSE), we have carried out a test calculation[64] on ([*Tm*$^{Bu^t}$]HgEPh complexes with neutral fragments. The BSSE errors for all three (S, Se, and Te containing) complexes are pretty much the same, which further gives confidence regarding the determined bonding energy sequence between Hg and chalcogens.

CONCLUSION

A systematic DFT investigation has been carried out on a variety of complexes containing Zn, Cd, and Hg to determine the chalcogenophilicity of Hg, keeping in the mind the recent work of Melnick et al.[25] The bond distances between Cd/Hg and the ligands depend on the specific nature of the ligands. With higher electronegativity of the ligands, for example, chloride, a more ionic type of bond is formed between those ligands and Cd/Hg. For the bonds that are of ionic type, the Cd-ligand bond distances are shorter than those of the corresponding Hg-ligand bonds. These trends are in accordance with the ionic radii of Cd and Hg, that is, the higher the ionic radius, the longer the bond. On the other hand, with ligands of lower electronegativity, for example, SH^{-}, Cd/Hg form bonds that are best characterized as covalent. In this type of bonding, the Cd-ligand bonds are longer than the corresponding Hg-ligand bonds in accordance with the covalent radii of Cd/Hg. This ionic and covalent character also dictates the bond distances in the [Tm^{Y}]MEZ complexes (Y = H, Me, Bu^{t}; M = Cd, Hg; E = S, Se, Te; Z = H, Ph). The M−E (E = Se, Te) bond

dx.doi.org/10.1021/ic200199b |*Inorg. Chem.* 2011, 50, 3791–3798

distance for Cd complexes increases from $Cd(EH)_4$ to $Cd(SH)_3EH$ complexes because of the higher ionic nature in the Cd−S bond; however, the opposite is observed for Hg because of the covalent nature of the bond between the Hg and E atoms. The shorter bond distance for Hg−Se and Hg−Te in $[Tm^{Bu^t}]$HgEPh is due to the higher covalent character (orbital interactions) between Hg and E (Se, Te), the crystal packing, and bulky groups present in the complexes. The BDE for Hg−E follows the same trend (Hg−S > Hg−Se > Hg−Te) for all compounds (with reasonable fragments) studied ranging from the smaller binary HgE molecules to the big $[Tm^{Bu^t}]$HgEPh complexes.

■ ASSOCIATED CONTENT

Supporting Information. Figure S1 showing M−E bond distances in $[M(EH)_4]^{2-}$ and $[M(SH)_3EH]^{2-}$; PES for HgE is shown in Figure S2; calculated electron affinities for EH and EPh (Table S1). This material is available free of charge via the Internet at http://pubs.acs.org.

■ AUTHOR INFORMATION

Corresponding Author

*E-mail: asaduzza@cc.umanitoba.ca (A.M.A.), schrecke@cc.umanitoba.ca (G.S.).

■ ACKNOWLEDGMENT

G.S. is grateful to Ignacio Vargas-Baca for helpful comments on the manuscript. We would like to acknowledge funding from The EJLB Foundation (http://www.ejlb.qc.ca/), The University of Manitoba (University Research Grants Program, URGP), and the Natural Sciences and Engineering Research Council of Canada (NSERC). Part of the quantum-mechanical calculations were enabled by the use of WestGrid computing resources, which are funded in part by the Canada Foundation for Innovation, Alberta Innovation and Science, BC Advanced Education, and the participating research institutions. WestGrid equipment is provided by IBM, Hewlett-Packard, and SGI.

■ REFERENCES

(1) WHO, *Environmental Health Criteria 101*; World Health Organization: Geneva, Switzerland, 1990.
(2) Harada, M. *Crit. Rev. Toxicol.* **1995**, *25*, 1–24.
(3) McAlpine, D.; Araki, S. *Lancet* **1958**, *2*, 629–631.
(4) Clarkson, T. W.; Magos, L. *Crit. Rev. Toxicol.* **2006**, *36*, 609–662.
(5) Mutter, J.; Naumann, J.; Guethlin, C. *Crit. Rev. Toxicol.* **2007**, *37*, 537–549.
(6) Clarkson, T. W. *Environ. Health Perspect. Suppl.* **2002**, *110*, 11-23.
(7) Clarkson, T. W. *Crit. Rev. Clin. Lab. Sci.* **1997**, *34*, 369–403.
(8) Boening, D. W. *Chemosphere* **2000**, *40*, 1335–1351.
(9) Alessio, L.; Campagna, M.; Lucchini, R. *Am. J. Ind. Med.* **2007**, *50*, 779–787.
(10) Tai, H.; Lim, C. *J. Phys. Chem. A* **2006**, *110*, 452–462.
(11) Rooney, J. P. K. *Toxicology* **2007**, *234*, 145–156.
(12) Paørízek, J.; Ošádalová, I. *Experientia* **1967**, *23*, 142–143.
(13) Cuvin-Aralar, M. L. A.; Furness, R. W. *Ecotoxicol. Environ. Saf.* **1991**, *21*, 348–364.
(14) Yang, D.-Y.; Chen, Y.-W.; M., G. J.; Belzile, N. *Environ. Rev.* **2008**, *16*, 71–92.
(15) Kaur, P.; Evje, L.; Aschner, M.; Syversen, T. *Toxicol. Vitro.* **2009**, *23*, 378–385.
(16) Arnold, A. P.; Tan, K.-S.; Rabenstein, D. L. *Inorg. Chem.* **1986**, *25*, 2433–2437.
(17) Rabenstein, D. L.; Tourangeau, M. C.; Evans, A. *Can. J. Chem.* **1976**, *54*, 2517–2525.
(18) Sugiura, Y.; Hojo, Y.; Tamai, Y.; Tanaka, H. *J. Am. Chem. Soc.* **1976**, *98*, 2339–2340.
(19) Sugiura, Y.; Tamai, Y.; Tanaka, H. *Bioinorg. Chem.* **1978**, *9*, 167–180.
(20) Asaduzzaman, A. M.; Khan, M. A. K.; Schreckenbach, G.; Wang, F. *Inorg. Chem.* **2010**, *49*, 870–878.
(21) Cremer, D.; Kraka, E.; Filatov, M. *Chem. Phys. Chem.* **2008**, *9*, 2510–2521.
(22) Filatov, M.; Cremer, D. *Chem. Phys. Chem.* **2004**, *5*, 1547–1557.
(23) Peterson, K. A.; Shepler, B. C.; Singleton, J. M. *Mol. Phys.* **2007**, *105*, 1139–1145.
(24) Khan, M. A. K.; Asaduzzaman, A.; Schreckenbach, G.; Wang, F. *Dalton Trans.* **2009**, 5766–5772.
(25) Melnick, J. G.; Yurkerwich, K.; Parkin, G. *J. Am. Chem. Soc.* **2010**, *132*, 647–655.
(26) *Chem. Eng. News* **2010**, *88*(2), 33.
(27) Laikov, D. N. *Chem. Phys. Lett.* **1997**, *281*, 151.
(28) Laikov, D. N. *Chem. Phys. Lett.* **2005**, *416*, 116–120.
(29) Laikov, D. N.; Ustynyuk, Y. A. *Russ. Chem. Bull.* **2005**, *54*, 820–826.
(30) Koch, W.; Holthausen, M. C. *A Chemist's Guide to Density Functional Theory*; Wiley-VCH: Weinheim. Germany, 2000.
(31) Perdew, J. P.; Burke, K.; Ernzerhof, M. *Phys. Rev. Lett.* **1996**, *77*, 3865–3868.
(32) Dyall, K. G. *J. Chem. Phys.* **1994**, *100*, 2118–2127.
(33) Asaduzzaman, A. M.; Schreckenbach, G. *Phys. Chem. Chem. Phys.* **2011**, submitted for publication.
(34) Schreckenbach, G.; Shamov, G. A. *Acc. Chem. Res.* **2010**, *43*, 19–29.
(35) Shamov, G. A.; Schreckenbach, G. *J. Phys. Chem. A* **2005**, *109*, 10961–10974. Correction note: Shamov, G. A.; Schreckenbach, G. *J. Phys. Chem. A* **2006**, *110*, 12072–12072.
(36) Shamov, G. A.; Schreckenbach, G.; Vo, T. *Chem.—Eur. J.* **2007**, *13*, 4932–4947.
(37) Ziegler, T.; Rauk, A. *Inorg. Chem.* **1979**, *18*, 1558–1565.
(38) Ziegler, T.; Rauk, A. *Inorg. Chem.* **1979**, *18*, 1755–1759.
(39) *ADF2008*; Department of Theoretical Chemistry, Vrije Universiteit: Amsterdam, The Netherlands, 2008.
(40) Baerends, E. J.; Ellis, D. E.; Ross, P. *Chem. Phys.* **1973**, *2*, 41–51.
(41) Fonseca Guerra, C.; Snijders, J. G.; te Velde, G.; Baerends, E. J. *Theor. Chem. Acc.* **1998**, *99*, 391–403.
(42) te Velde, G.; Baerends, E. J. *J. Comput. Phys.* **1992**, *99*, 84–98.
(43) Versluis, L.; Ziegler, T. *J. Chem. Phys.* **1988**, *88*, 322–328.
(44) van Lenthe, E.; Snijders, J. G.; Baerends, E. J. *J. Chem. Phys.* **1996**, *105*, 6505.
(45) van Lenthe, E.; van Leeuwen, R.; Baerends, E. J.; Snijders, J. G. *Int. J. Quantum Chem.* **1996**, *57*, 281.
(46) Allen, F. H.; Kennard, O. *Chem. Des. Autom. News* **1993**, *8*, 1 & 31–37.
(47) Peterson, K. A.; Figgen, D.; Dolg, M.; Stoll, H. *J. Chem. Phys.* **2007**, *126*, 124101.
(48) Gorelsky, S. I.; Basumallick, L.; Vura-Weis, J.; Sarangi, R.; Hodgson, K. O.; Hedman, B.; Fujisawa, K.; Solomon, E. I. *Inorg. Chem.* **2005**, *44*, 4947–4960.
(49) Roy, G.; Sharma, B. K.; Phadnis, P. P.; Mugesh, G. *J. Chem. Sci.* **2005**, *117*, 287–303.
(50) Capps, K. B.; Wixmerten, B.; Bauer, A.; D., H. C. *Inorg. Chem.* **1998**, *37*, 2861–2864.
(51) McDonough, J. E.; Weir, J. J.; Sukcharoenphon, K.; D., H. C.; Kryatova, O. P.; Rybak-Akimova, E. V.; Scott, B. L.; Kubas, G. J.; Mendiratta, A.; Cummins, C. C. *J. Am. Chem. Soc.* **2006**, *128*, 10295–10303.
(52) González-Blanci, O.; Branchadell, V.; Monteyne, K.; Ziegler, T. *Inorg. Chem.* **1998**, *37*, 1744–1748.
(53) McDonough, J. E.; Mendiratta, A.; Curley, J. J.; Fortman, G. C.; Fantasia, S.; Cummins, C. C.; Rybak-Akimova, E. V.; Nolan, S. P.; Hoff, C. D. *Inorg. Chem.* **2008**, *47*, 2133–2141.

(54) Schumann, H.; Arif, A. M.; Rheingold, A.; Janiak, C.; Hoffmann, R.; Kuhn, N. *Inorg. Chem.* **1991**, *30*, 1618–1625.
(55) Hoffmann, R. *J. Chem. Phys.* **1963**, *39*, 1397.
(56) Hoffmann, R.; Lipscomb, W. N. *J. Chem. Phys.* **1962**, *36*, 2179.
(57) Hoffmann, R.; Lipscomb, W. N. *J. Chem. Phys.* **1962**, *37*, 2872.
(58) http://www.webelements.com/.
(59) Cordero, B.; Gómez, V.; Platero-Prats, A. E.; Revés, M.; Echeverría, J.; Cremades, E.; Barragán, F.; Alvarez, S. *Dalton Trans.* **2008**, 2832–2838.
(60) Cameron, A. F.; Forrest, K. P.; Ferguson, G. J. *J. Chem. Soc. A* **1971**, 1286–1289.
(61) Lobana, T. S.; Sandhu, M. K.; Snow, M. R.; Tiekink, E. R. T. *Acta Crystallogr.* **1988**, *C44*, 179–181.
(62) Wulfsberg, W. *Inorganic Chemistry*; University Science Books: Sausalito, CA, 2000.
(63) Bickelhaupt, F. M.; Baerends, E. J. In *Reviews in Computational Chemistry*; Lipkowitz, K. B., Boyd, D. B., Eds.; Wiley-VCH: New York, 2000; Vol. 15.
(64) The counterpoise calculations were carried out using the g03 program with the PBE functional. The basis sets 6-31+G* for H, C, B, N, 6-311+G* for S and Se and SDD with effective core potential for Te and Hg were used.